JOURNAL OF Materials CHEMISTRY

$AA'_2M_3O_{10}$ (A = K, Rb, Cs; A′ = Ca; M = Nb) layered perovskites: low-temperature proton conductors in hydrogen atmospheres

Venkataraman Thangadurai and Werner Weppner*

Faculty of Engineering, Chair for Sensors and Solid State Ionics, Christain-Albrechts University, Kaiserstr. 2, D-24143 Kiel, Germany. Fax: +49 431 77572 553; E-mail: ww@tf.uni-kiel.de

Received 17th August 2000, Accepted 26th October 2000
First published as an Advance Article on the web 2nd January 2001

Electrical conductivity of the Dion–Jacobson (D–J) type layered perovskite oxides, $AA'_2M_3O_{10}$ (A = K, Rb, Cs; A′ = Ca; M = Nb, Ta), is determined by AC impedance analysis in hydrogen atmospheres and in air. The electrical conductivity behavior of the layered perovskite oxides in hydrogen is different from that in air. Among the layered perovskites, $KCa_2Nb_3O_{10}$ exhibits the highest electrical conductivity, σ, of 3.2×10^{-4} S cm^{-1} at 45 °C with an activation energy, E_a, of 0.25 eV in a hydrogen atmosphere. Open circuit voltage measurements at room temperature with hydrogen–oxygen gas concentration cells reveal that the mobile charge carriers are most likely protonic in origin. The electrical (proton) conductivity is comparable to that of fast lithium ionic conductors based on the perovskite structure such as (Li,La)TiO_3 at the same temperature.

1. Introduction

Among the various mono-valent ions with fast-ion transport in solid state ionic conductors, protons play a special role in view of their size and possible applications.[1] The present interest in solid proton conductors includes energy conversion in fuel cells, electrolytic cells, the sensing of hydrogen, ammonia or water, hydrogen pumps and the determination of fundamental thermodynamic and kinetic quantities of solids with hydrogen as one of the constituents. In general, solid state proton conductors (SSPCs) are being classified according to the preparation method, structural dimensions and operating temperatures.[2] With regard to the temperature, SSPCs are classified into two types, (i) low-temperature and (ii) high-temperature conductors. Inorganic metal oxide hydrates[3] ($SnO_2\cdot2H_2O$, $V_2O_5\cdot nH_2O$) and solid acids, hydrogen uranyl phosphate,[4] $H_3OUO_4PO_4\cdot3H_2O$ and phosphotungstic acid,[5] $H_3PW_{12}O_{40}\cdot nH_2O$ (n = 21–29) are examples of low-temperature proton conductors. Acceptor-doped 3D perovskites,[6–9] (Sr,Ba)(Zr,Ce)O_3, and rare earth oxides[10,11] (Gd_2O_3, Dy_2O_3, Er_2O_3, Y_2O_3) which may exhibit proton conduction in hydrogen containing atmospheres at elevated temperature (> 600 °C) are typical examples of high temperature proton conductors. The proton conduction in these oxides is considered to be due to the following defect reactions at high temperature in the Kröger–Vinck notation[12]

$$H_2O + V_o^{\cdot\cdot} + O_o^{\times} \rightleftharpoons 2[OH]_o^{\cdot} \quad (1)$$

where $V_o^{\cdot\cdot}$, $O_o^{\times}$ and $[OH]_o^{\cdot}$ represent oxygen vacancies created by the trivalent ion substitution for the regular tetravalent ion, oxygen and proton attached to the lattice (structural) oxygen. Hence, oxygen vacancies and water vapor are essential for the proton conduction.[6–9] It is assumed that the proton conduction occurs by the migration of hydroxyl ($OH_o^{\cdot}$) groups by the Grotthuss mechanism.[1,13] However, there is a competing electronic (hole) and oxide ion conduction in various gas atmospheres and at various temperatures.[6–9]

Interesting examples of both low- and high-temperature proton conductors are based on the layered perovskite oxides. For example, the n = 2 member of the D–J series,[14,15] $HLaNb_2O_7\cdot nH_2O$,[16,17] is the typical example for the low temperature SSPC and n = 3 member of the Ruddlesden–Popper (R–P) series;[18] $H_2Ln_2Ti_3O_{10}$ (Ln = rare earth) oxides are examples of high temperature SSPCs.[19] These layered perovskite oxides were obtained from their corresponding alkali analogues by ion exchange reaction using acids. The proton conduction occurs, however, in the first case along the surface of the grains. In the latter case, the electrical conduction is most likely due to proton conduction in the anion-deficient layered perovskite, $Ln_2Ti_3O_9$, which is formed *in situ* at temperatures above 200 °C. Thus, the observed proton conduction is analogous to that of acceptor-doped anion deficient (Sr,Ba)CeO_3 perovskites.[19] However, the corresponding alkali analogue layered perovskites exhibit ionic conduction. For example, the n = 2 member[16] of the D–J series, $NaLaNb_2O_7$, exhibits an ionic conductivity[20] of 1.80×10^{-4} S cm^{-1} at 600 °C with an activation energy of 0.30 eV (300–600 °C) for sodium ion conduction.

An interesting aspect of these materials is that there is structural similarity to the well-known layered compounds most extensively studied by many laboratories, the so-called beta-aluminas,[21] which are finding applications in many solid state devices such as high temperature batteries and sensors for various gases.[22] Both layered perovskites and beta-alumina are 2D-layered materials, the alkali metal ions lie in-between the perovskites or spinel blocks. The electrical ionic conductivity is due to the migration of alkali metal ions in the interlayer conduction paths. In view of the structural similarity, we explore the possible electrochemical applications of the n = 3 member D–J layered perovskites. In our primary investigations, we found that $RbCa_2Nb_3O_{10}$[14] exhibits an unusual increase in the electrical current in the amperometric limiting current sensors for ammonia gas at 400 °C. We realized that the observed current is likely to be due to the proton migration in this material since ammonia is unstable at this temperature. Indeed, as we expected, D–J series oxides exhibit much higher conductivity in hydrogen atmospheres. For example, $KCa_2Nb_3O_{10}$ exhibits an electrical conductivity of 3.2×10^{-4} S cm^{-1} with an activation energy of 0.25 eV at 45 °C in a hydrogen atmosphere. The conductivity value is much higher than that of the 3D-acceptor doped perovskites[6–9] and comparable to many 3D materials exhibiting mono-valent ionic conduction such as NASICONs[23] and LISICONs.[24]

 DOI: 10.1039/b006750o

2. Experimental aspects

D–J layered perovskite oxides of the general formula $AA'_2M_3O_{10}$ (A = K, Rb, Cs; A′ = Ca; M = Nb, Ta) were prepared by using solid state reactions of appropriate mixtures of ANO_3, $CaCO_3$, Nb_2O_5 and Ta_2O_5 obtained from Fluka or Aldrich (purity > 99.9%) at elevated temperatures in alumina crucibles.[14,15] 20 wt% excess alkali metal carbonates or nitrates were added to avoid any loss of alkali metal ion during the synthesis. Any excess alkali was removed by washing with water. The powder samples were characterized with regard to phase formation by powder X-ray diffraction (XRD) using a Siemens-D5000 powder X-ray diffractometer (CuKα) at room temperature. The powders were made into compact cylinders by isostatic pressing at 38 kN cm^{-2} and sintering in air at the same temperature at which the polycrystalline samples were synthesized. The sintered cylinders were cut into thin coin-type pellets (~1.2 mm thick with 10 mm diameters) suitable for the electrical measurements.

The pellet surfaces were pasted with platinum paste and annealed at 850 °C for 1 h. Impedance data were obtained in the temperature range 50–750 °C using an HP4192A HP impedance bridge in the frequency range 5 Hz–13 MHz in air and hydrogen atmospheres. Prior to all impedance measurements, the samples were kept at constant temperature for a minimum of about 6–9 h. Electrical conductivity data were obtained from the low-frequency minimum of the impedance plot. Open-circuit potentials of the galvanic cells were measured using a digital electrometer (10^{14} Ω, Ionic Systems).

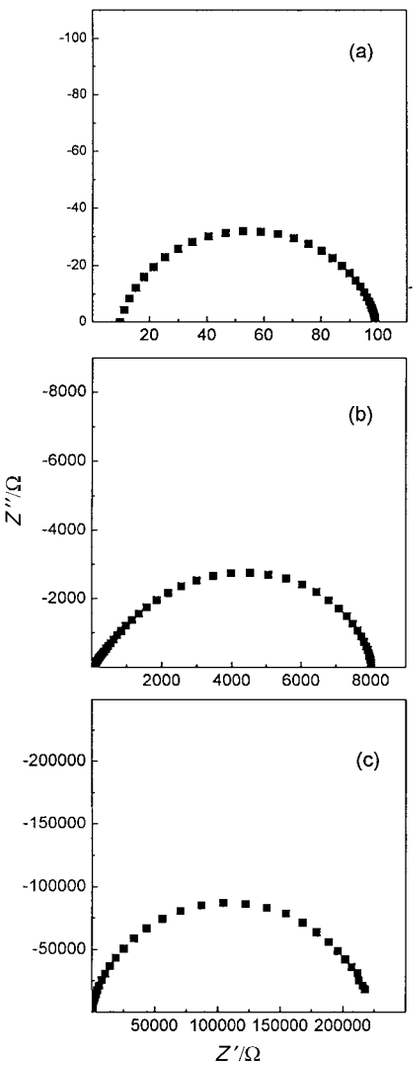

Fig. 1 Impedance plots obtained at 100 °C in a hydrogen atmosphere from the second cooling cycle: (a) $KCa_2Nb_3O_{10}$, (b) $RbCa_2Nb_3O_{10}$, and (c) $CsCa_2Nb_3O_{10}$.

3. Results and discussion

The phase formation of the layered perovskites was confirmed by comparison of the powder X-ray diffraction patterns (XRD) and the lattice parameters with literature data. Electrical conductivity values obtained using the AC impedance method in air are comparable to similar values available in the literature. As expected, the conductivity behavior of the layered perovskites in hydrogen gas is distinctly different from the air data. Typical impedance plots obtained in a hydrogen atmosphere at 100 °C are shown in Fig. 1. We see simple single semicircles with no visible low frequency tails. This indicates a simple parallel resistance–capacitance analog. This observation is typical for the ionic conducting material with non-blocking electrodes. However, at 100 °C in air, we did not observe semicircles suggesting that the impedance of the sample decreased under the hydrogen atmosphere.

Arrhenius plots for the electrical conduction of $ACa_2Nb_3O_{10}$ (A = K, Rb, Cs) in hydrogen gas together with air data are shown in Figs. 2–4. There is a strong, but continuous, increase in the electrical conduction at around 150 °C. We see conductivity values several orders of magnitude higher than in air. The conductivity value obtained from the first cooling and heating at different steps follows the same line indicating the true conductivity behavior of the samples. Among the series, $KCa_2Nb_3O_{10}$ exhibits the highest conductivity of 3.2×10^{-4} S cm^{-1} which is much higher than that of the corresponding Rb- and Cs-analogues. This finding is similar to

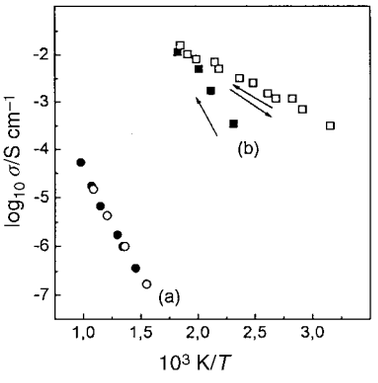

Fig. 2 Arrhenius plots for electrical conduction of $KCa_2Nb_3O_{10}$: (a) in air and (b) in a hydrogen atmosphere. The closed data points represent the heating cycle and the open data points represent the cooling cycle.

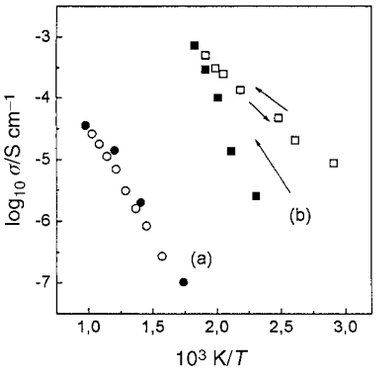

Fig. 3 Arrhenius plots for electrical conduction of $RbCa_2Nb_3O_{10}$: (a) in air and (b) in a hydrogen atmosphere. The closed data points represents the heating cycle and the open data points represent the cooling cycle.

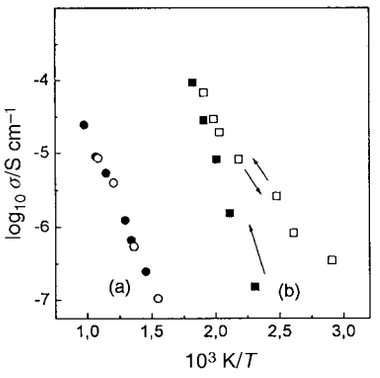

Fig. 4 Arrhenius plots for electrical conduction of $CsCa_2Nb_3O_{10}$: (a) in air and (b) in a hydrogen atmosphere. The closed data points represents the heating cycle and the open data points represent the cooling cycle.

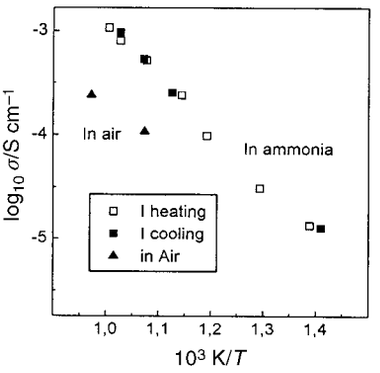

Fig. 5 Arrhenius plots for electrical conduction of $KCa_2Ta_3O_{10}$ in air and in 1000 ppm ammonia.

that found in air. The difference in the electrical conductivity value lies possibly in the small structural difference across the series. Table 1 summarizes the electrical conductivity data of layered perovskites both in air and hydrogen. We assume that layered perovskites, $ACa_2Nb_3O_{10}$, may not contain defects such as oxygen vacancies due to alkali evaporation during the synthesis. It may be compensated by excess alkali added during the synthesis. Even if oxygen vacancies exist in the investigated temperature range (50–300 °C) its contribution to the total conductivity will be negligibly small. Thus, we believe that the observed high electrical conductivity in hydrogen is most likely due to proton conduction in the layered perovskites.

To our knowledge, the proton conduction in oxides that do not contain oxygen vacancies has not been reported, except for off-stoichiometric $Ba_3CaNb_2O_9$ which exhibits proton conductivity[25] that is comparable to Nd-doped $BaCeO_3$.[10] We believe that in the present investigation a similar conductivity mechanism is applicable since the layered perovskite contains neither oxygen vacancies nor protons. However, further clarification on the mechanism of proton conduction is nescessary.

We see a similar increase in the electrical conductivity behavior in 1000 ppm ammonia gas in argon for the D–J series of $ACa_2Nb_3O_{10}$ layered perovskites. For the purposes of comparison we measured the electrical conductivity of one of the Ta-compounds, $KCa_2Ta_3O_{10}$, in a 1000 ppm ammonia atmosphere. Unlike $ACa_2Nb_3O_{10}$, the corresponding Ta-compound[26] $KCa_2Ta_3O_{10}$ exhibits a small increase in the electrical conduction in ammonia as compared to air. The conductivity obtained from the first heating and cooling cycle falls on the same line with an activation energy of 0.96 eV (Fig. 5). We have measured the electrical conductivity of $K_2La_2Ti_3O_{10}$,[27] an $n=3$ member of the R–P series, in a hydrogen atmosphere for the purposes of comparison and the data are shown in Fig. 6. The conductivity value is similar to that of the Cs-compound, $CsCa_2Nb_3O_{10}$. The conductivity is much less than for the corresponding K-analogue, $KCa_2Nb_3O_{10}$. The result is consistent with the interlayer cation density and the conductivity behavior of the layered perovskites. It is known that the D–J series has lower interlayer cation density than the R–P series, favorable for ionic conduction in-between the perovskite slabs, hence it is most likely that the D–J series exhibits much higher conductivity in both air and hydrogen atmospheres.

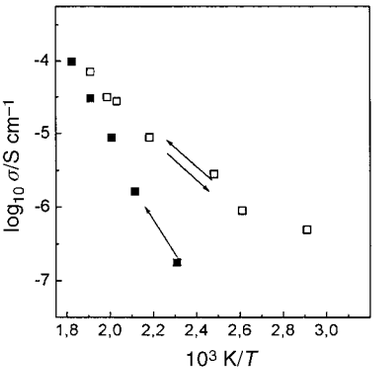

Fig. 6 Arrhenius plots for electrical conduction of $K_2La_2Ti_3O_{10}$ in a hydrogen atmosphere. The closed data points represent the heating cycle and the open data points represent the cooling cycle.

We also investigated the effect of water vapor on the electrical conductivity of $KCa_2Nb_3O_{10}$ by passing humidified argon gas (the argon gas was humidified by bubbling through hot water, maintained at 100 °C using an oil bath) over the sample. We see that there is no influence on the electrical conduction (Fig. 7). This result is not surprising since the layered perovskite material does not contain oxygen vacancies and hence we would not expect interaction of water vapor as described in eqn. (1).

The results suggest that Nb-compounds are most likely being reduced in a hydrogen atmosphere resulting in electronic conduction or the generation of oxygen vacancies which favors

Table 1 Electrical conductivity data of the layered perovskites, $AA'_2M_3O_{10}$ (A = K, Rb, Cs; A′ = Ca; M = Nb) and $K_2La_2Ti_3O_{10}$

Compound	$\sigma_{700\,^\circ C,air}$/S cm^{-1}	$\sigma_{270\,^\circ C,H_2}$/S cm^{-1}	E_{a,H_2}/eV	$E_{a,air}$/eV
$KCa_2Nb_3O_{10}$	5.6×10^{-5}	1.53×10^{-2}	0.25	0.89
$RbCa_2Nb_3O_{10}$	4.2×10^{-5}	7.76×10^{-4}	0.34	0.73
$CsCa_2Nb_3O_{10}$	1.0×10^{-4}	9.40×10^{-5}	0.44	0.58
$K_2La_2Ti_3O_{10}$	—	9.00×10^{-5}	0.44	—

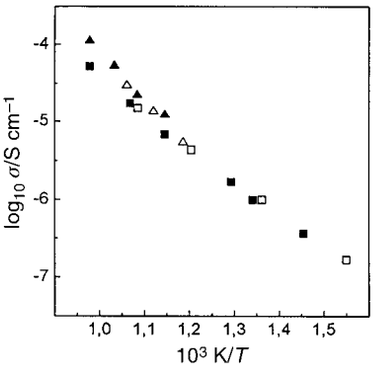

Fig. 7 Arrhenius plots for electrical conduction of $KCa_2Nb_3O_{10}$, in air (open and closed squares) and in humidified argon gas (open and closed triangles). The closed data points represent the heating cycle and the open data points represent the cooling cycle.

Table 2 Stable EMF (open circuit voltage) for the galvanic cell using $KCa_2Nb_3O_{10}$ as electrolyte at room temperature

Cell	EMF/mV
Air ‖ air, H_2O	4
Air (bubbled) ‖ air, H_2O	37
NH_3 (1000 ppm) ‖ air, H_2O	−180
H_2 ‖ air, H_2O	−920
H_2 |blue colored sample| air, H_2O	−580

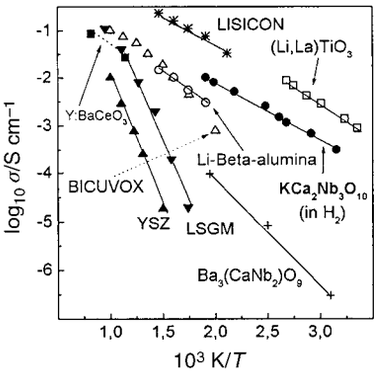

Fig. 8 Comparison of the electrical conductivity data of $KCa_2Nb_3O_{10}$ obtained in a hydrogen atmosphere with well-known oxide, lithium and high temperature proton conductors reported in the literature.

proton conduction similar to that of acceptor doped-3D perovskites. However, we do not see any significant change in weight during the thermogravimetric experiments using hydrogen gas up to 750 °C (1 °C min^{-1}). The compounds are slightly blue in color at the surface after the electrical conductivity measurements. So the possible electronic contribution to the total ionic conduction may be present in only small amounts. Further investigations are needed, however, to quantify the contribution of electronic conductivity to the total conductivity.

Table 2 lists the stable EMF for different galvanic cells utilizing $KCa_2Nb_3O_{10}$ as electrolyte. In all cases, the electrode with higher hydrogen activity has the negative polarity. The difference in the hydrogen partial pressure between the electrodes can be due to the following electrode reactions:

$$H_2 \rightarrow 2H^+ + 2e^- \text{ at the hydrogen side (anode)}$$

$$2H^+ + {}^1/_2O_2 + 2e^- \rightarrow H_2O \text{ at the air side (cathode)}$$

It is interesting to note that the blue colored sample also shows a stable EMF of −580 mV under similar conditions. For electronic conduction, one would not observe any stable EMF. Hence, the observed EMF/conductivity is most likely ionic/protonic in nature.

Fig. 8 compares the electrical conductivity data of $KCa_2Nb_3O_{10}$ obtained from the second cycle in a hydrogen atmosphere. We see that at low temperature the conductivity is much higher than some of the well-known perovskite oxide ion conductors LSGM,[28] high temperature proton conductors based on the acceptor doped-$BaCeO_3$,[6–9] $Ba_3(CaNb_2)O_9$.[25] The conductivity is comparable to that of the NASICONs,[23] Li-β-alumina and lithium ion conductors based on the perovskite $(Li,La)TiO_3$.[29] Further work is in progress to use these material as electrolytes in galvanic cell applications, such as sensors for hydrogen, and ammonia gas sensors at low temperature.

4. Conclusions

Layered perovskites of the Dion–Jacobson (D–J) type, $AA'_2Nb_3O_{10}$ (A = K, Rb, Cs; A′ = Ca), exhibit unusual electrical properties in hydrogen atmospheres. Among the oxides investigated, $KCa_2Nb_3O_{10}$ exhibits the highest ionic conductivity of 3.2×10^{-4} S cm^{-1} at 45 °C, which is comparable to some of the cation and anion conductors based on the perovskite structure. We see that electrical conduction depends on the hydrogen and ammonia concentration which suggests that these layered oxides may be potential candidates for hydrogen and ammonia gas sensors.

Acknowledgements

The authors would like to thank Prof. T. Norby for helpful discussions, and Dr W. F. Chu for assistance in the TGA measurements. We also thank Dr Peter Schmid-Beurmann, Institut fuer Geowissenschaften, Kiel for providing time and assistance for the powder X-ray diffraction measurements.

References

1 K. D. Kreuer, *Chem. Mater.*, 1996, **8**, 610.
2 P. Colomban and A. Novak, in *Proton Conductors Solids, Membranes and Gels, Materials, and Devices*, P. Colomban (Editor), Cambridge Press, New York, 1992.
3 W. A. England, M. G. Cross, A. Hammett, P. J. Wiseman and J. B. Goodenough, *Solid State Ionics*, 1980, **1**, 231.
4 A. T. Howe and M. G. Shilton, *Mater. Res. Bull.*, 1977, **12**, 701.
5 O. Nakamura, I. Ogino and T. Kodama, *Solid State Ionics*, 1981, **3–4**, 347; K. D. Kreuer, M. Hampele, K. Dolde and A. Rabenau, *Solid State Ionics*, 1988, **28–30**, 589.
6 H. Iwahara, T. Esaka, H. Uchida and N. Maeda, *Solid State Ionics*, 1981, **3–4**, 359.
7 H. Iwahara, *Solid State Ionics*, 1988, **28–30**, 573.
8 N. Bonanos, *Solid State Ionics*, 1992, **53–56**, 967.
9 S. V. Bhide and A. V. Virkar, *J. Electrochem. Soc.*, 1999, **146**, 4386.
10 T. Norby and P. Kofstad, *Solid State Ionics*, 1986, **20**, 169.
11 Y. Larring and T. Norby, *Solid State Ionics*, 1995, **77**, 147.
12 F. A. Kröger, *The Chemistry of Imperfect Crystals*, vol. 2, 2nd edition, North-Holland Publications, Amsterdam, 1974.
13 K. D. Kreuer, E. Schonherr and J. Maier, *Solid State Ionics*, 1994, **70–71**, 278.
14 M. Dion, M. Ganne and M. Tournoux, *Mater. Res. Bull.*, 1981, **16**, 1429.
15 A. J. Jacobson, J. T. Lewandowski and J. W. Johnson, *J. Less-Common Met.*, 1996, **116**, 137.
16 J. Gopalakrishnan, V. Bhat and B. Raveau, *Mater. Res. Bull.*, 1987, **22**, 413.
17 M. Sato, T. Jin and K. Uematsu, *J. Solid State Chem.*, 1993, **102**, 557.
18 S. N. Ruddlesden and P. Popper, *Acta Crystallogr.*, 1957, **10**, 538; S. N. Ruddlesden and P. Popper, *Acta Crystallogr.*, 1958, **11**, 54.
19 V. Thangadurai, A. K. Shukla and J. Gopalakrishnan, *Solid State Ionics*, 1994, **73**, 9.
20 M. Sato, J. Abo, T. Jin and M. Ohta, *J. Alloys Compd.*, 1993, **192**, 81.
21 G. Farrington and D. L. Briant, *Science*, 1979, **204**, 1371; R. Stevens and J. G. P. Binner, *J. Mater. Sci.*, 1984, **19**, 695; A. R. West, *Solid State Chemistry and its Applications*, John Wiley & Sons, New York, 1984, p. 467.
22 J. Jiu and W. Weppner, *Solid State Commun.*, 1990, **67**, 311; T. Widmer, V. Brüser, O. Schäf and U. Guth, *Ionics*, 1999, **5**, 86.
23 H. Y. P. Hong, *Mater. Res. Bull.*, 1976, **11**, 173; J. B. Goodenough, H. Y. P. Hong and J. A. Kafalas, *Mater. Res. Bull.*, 1976, **11**, 203.
24 P. G. Burce and A. R. West, *J. Solid State Chem.*, 1982, **44**, 354.
25 A. S. Nowick and Y. Du, *Solid State Ionics*, 1995, **77**, 137.
26 K. Toda, T. Teranishi, Z. G. Ye, M. Sato and Y. Hinatsu, *Mater. Res. Bull.*, 1999, **34**, 971.
27 J. Gopalakrishnan and V. Bhat, *Inorg. Chem.*, 1987, **26**, 4299.
28 T. Ishihara, H. Matsuda and Y. Takita, *J. Am.Chem. Soc.*, 1994, **116**, 3801; M. Feng and J. B. Goodenough, *Eur. J. Solid State Inorg. Chem.*, 1994, **31**, 663.
29 Y. Inaguma, L. Chen, M. Itoh, T. Nakamura, T. Uchida, H. Ikuta and M. Wakihara, *Soild State Commun.*, 1993, **86**, 689.